Determination of proton radii and neutron skin thickness of p-sd shell nuclei by Charge Changing Cross Section measurement.

Spokespersons : R. Kanungo[1] and I. Tanihata[2]
GSI Contact Person : C. Nociforo[3]
Collaboration :
H. Al Falou[1,5], A.T. Gallant[4,5], H. Geissel[3], K. Hirota[2], R. Janik[6], J. Kurcewicz[3], Y. Litvinov[3], C. Nociforo[3], H. J. Ong[2], S. Pietri[3], A. Prochazka[3], C. Scheidenberger[3], B. Sitar[6], P. Strmen[6], T. Suzuki[2], I. Szarka[6], A. Tamii[2], M. Uchida[1], H. Weick[3], M. Winkler[3]

[1]Saint Mary's University, Halifax, Nova Scotia, Canada
[2] Research Center for Nuclear Physics, Ibaraki, Osaka, Japan
[3]GSI, Darmstadt, Germany
[4]University of British Columbia, Vancouver, British Columbia, Canada
[5]TRIUMF, Vancouver, British Columbia, Canada
[6]Commenius University, Bratislava, Slovakia

SUMMARY OF THE PROPOSAL

We propose to measure the charge changing cross sections (CCCS, σ_{cc}) of B,C,O isotopes using radioactive beams of energies around 900*A* MeV. The CCCS is the total cross section for the change of the atomic number of projectile nucleus. We have been studying interaction cross sections, that is the total cross section of nucleon change in a projectile, and have been determining the root-mean-square matter radii as well as the matter density distributions. Similarly, CCCS is closely related to the distribution of protons in a nucleus. We consider that the recent progress of Glauber model analysis enables the extraction of the proton distribution radii of neutron rich nuclei.

One can deduce the thickness of neutron skin from a difference of the radii of nucleon distribution and proton distribution. Present proposal aims to study the systematic change of the neutron skin thickness in these isotopes. Such data would provide a means to distinguish nuclear models for very light nuclei where several new structure models including ab-initio type nuclear models are being introduced. Particular interests exist in B and C isotopes in which interplay between cluster structure and shell model structure plays an important role. For the O isotopes investigating the closed shell feature is of interest specially with a new magic number N=16 at the neutron-drip line. Different shapes between proton and neutron distribution is also among the interests from a view point of nuclear structure. The new structure models being developed require data of matter and charge radii to test their validity and understand the physical basis.

The experiment is planned to be performed at the final focus of the fragment separator FRS. The relativistic beams of neutron-rich isotopes that are unique to GSI are the best suited for achieving the goals of this experiment both from theoretical interpretation as well as experimental point of view.

1. Scientific Motivation

Radii of nucleon distribution in nuclei (we simply call this as matter radii in the following) have been extensively measured for unstable nuclei and revealed new structures in nuclei far from the stability line. One of the most interesting questions along this direction is the difference between radii of the protons and neutrons distribution in a nucleus. (We call those as proton radius and neutron radius unless explicitly specified.) Theoretical model calculations indicate that the systematic study of neutron skin thickness is a very sensitive tool to study the isospin dependence of nuclear matter equation of state (EOS). In light nuclei, recently developing new ab-initio type nuclear models, such as Green's function Monte-Carlo, AMD and No-core shell model can be sensitively tested by the proton and neutron distributions. For example the AMD model predicts appearances and disappearances of cluster structures and thus predicts characteristic change of proton and neutron radii.[1] It is also an interesting question whether protons and neutrons can have different deformations. Another important information one can obtain is the correlation of neutrons in extremely neutron rich nuclei. Recent measurements of the charge radii of halo nuclei (^{6}He [2] and ^{11}Li [3]) showed the increase of the charge radii due to the halo formation. It shows the possibility of sensitive study of two-halo neutron correlations from the radii. It is therefore clear that determination of proton and matter radii of nuclei far from stability are of great importance.

Investigations over the past decade have pointed out that neutron (or proton) skins exist in nuclei far from the stability line. The first direct evidence has been discovered in Na isotopes by comparing the charge radii determined by isotope shift measurements and the matter radii determined by interaction cross section measurements. [4] However Na was the lightest isotopes of which charge radii could be extracted from isotope shift measurement at that time. Determining isotope shifts for all isotopic chains is still a challenge. Matter radii have been measured systematically for light nuclei where isotopic chains are accessible to very neutron-rich regions. It is therefore very important to determine the charge radii in this region.

The determination of charge radii of light nuclei from isotope shift was impossible until recently. It was not because of the precision of the measurement itself but due to the accuracy of theoretical calculations of the mass shift. The mass shift has to be subtracted from the measured shift to obtain the difference of charge distributions. The mass shift is orders of magnitude larger than the shift due to the change in charge radii and can not be determined by the measurement. It is also related to the correlation between atomic electrons. Only very recently, spectacular developments have been made in atomic calculations in the lightest elements, He and Li. [5] Recently charge radii of all He and Li isotopes have been determined by precise isotope shift measurements with the help of the new atomic physics calculations as well as precise new mass measurements.

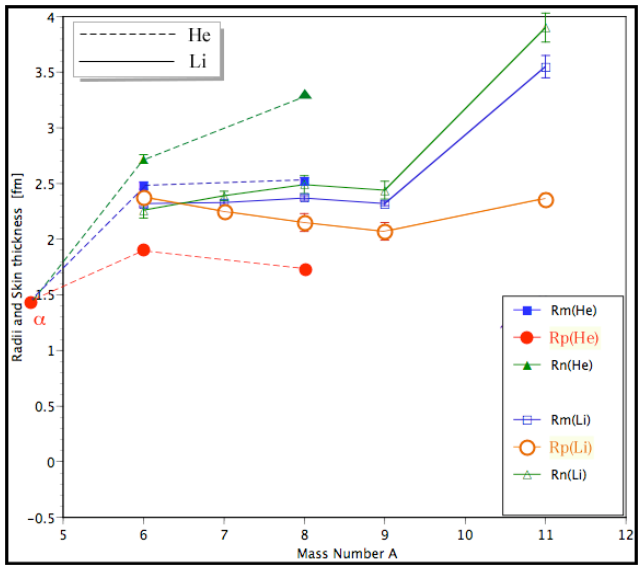

Fig. 1 Matter, proton, and neutron radii of He and Li isotopes.
Li: R. Sanchez et al., Phy. Rev. Let. **96** (2006) 033002.
^{6}He: L. -B. Wang et al., Phys. Rev. Let. **93** (2004) 142501.
^{8}He: P. Mueller et al., Phys. Rev. Let. **99** (2007) 252501.
Matter radii: A. Ozawa et al., Nucl. Phys. A **693** (2001) 32.

However, the extension of isotope shift measurements is difficult for very neutron-rich isotopes of Be, B, C, N, O, and F. The difficulty is two fold, one is the difficulty of high-precision

isotope shift measurements. This is due to the difficulty in producing enough number of cooled beam of short lived isotopes of such elements. The other is again difficulties in atomic physics calculation due to many-body correlations between electrons in atoms.

The Isotope shift measurements showed that the proton radii of ^{6}He and ^{11}Li increases from the proton radii of the core nuclei ^{4}He and ^{9}Li, respectively. (Fig. 1) Since core+n+n model works very well for those nuclei, the larger proton radius can be understood as due to a motion of a core nucleus around the center of mass of a halo nucleus. The center of mass motion is directly related to the correlation of two halo neutrons. Therefore, the matter radius and the proton radius of a two-neutron halo nucleus provide one important direction for studying some aspects of the correlation of neutrons neutron-rich nuclei. A comparison of proton radii of ^{6}He, ^{11}Li, ^{14}Be, ^{17}B would be extremely interesting in view of the correlation because they are Borromean nuclei but the contributing orbitals in halos are progressively different, namely only p-wave in ^{6}He but p- and s-waves in ^{11}Li and p-, s-, d-waves in ^{14}Be and s- and d- waves in ^{17}B. Importance of di-neutron correlation is of great interest as well.

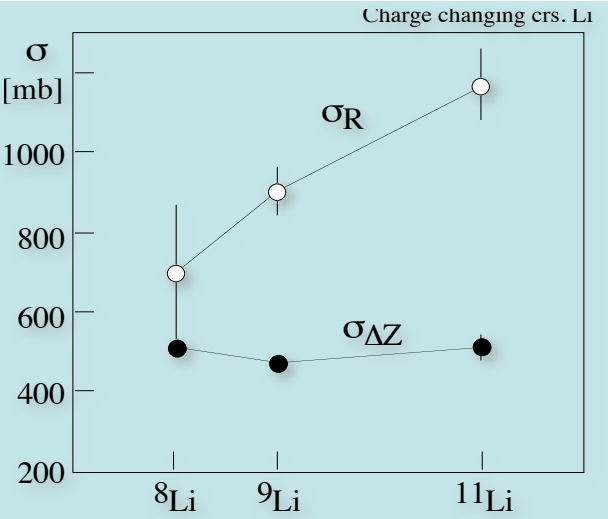

Fig. 2 Reaction cross section and charge changing cross sections of Li isotopes. [6]

It was considered that the proton radius would be impossible to determine by strong interaction probes. However we now know that the geometrical model, in particular Glauber model works very well also for charge changing cross sections (CCCS). Charge changing cross sections have been measured for Li isotopes[6] (Fig. 2) some time ago at around 80*A* MeV. In this data, the CCCS decreases from ^{8}Li to ^{9}Li but increases from ^{9}Li to ^{11}Li. The change of charge changing cross section being much smaller than the dramatic change of interaction cross section, the observation but was not viewed deeply at that time. New isotope shift measurements confirmed the same trend of charge radii in Li isotopes and thus, in one way, provide a confirmation of the geometrical understanding of the CCCS. As will be discussed in the next section we find that the charge radius that can be extracted from the CCCS data is in agreement with the observations from isotope shift.

The CCCS of B, C, N, O isotopes have been measured at GSI (Fig. 3). In general, this showed that the σ_{cc} changes slightly for neutron-rich B isotopes, while the C and O isotopes does not change much when neutron number is changed [7]. It might be suggesting that the proton radius does not increase significantly for neutron rich isotopes indicating the development of neutron skin. However when these data for the stable nucleus of each isotopic chain are compared with earlier data [8] from Berkeley there appears to be a systematic inconsistency. A Glauber model calculation seems to be

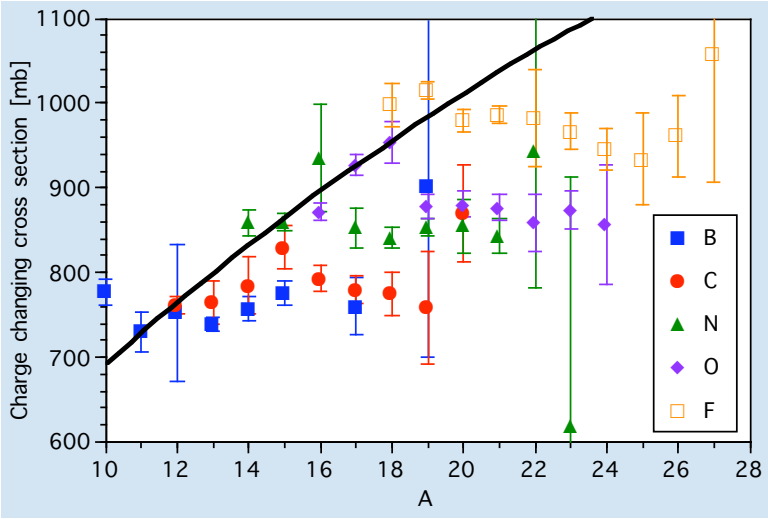

Fig. 3 Charge changing cross sections measured at GSI. [7]

consistent with the data in Ref.[8] as will be shown in the following section. Moreover the uncertainties of the σ_{cc} specially for the very neutron-rich isotopes such as ^{17}B, $^{19\text{-}20}$C and ^{23,24}O are so large that a meaningful discussion on the evolution of charge radii and hence on the neutron skin is not possible. It is therefore necessary to determine the σ_{cc} with precision < 2% that is comparable to the precision of interaction cross sections and allows a meaningful comparison to predictions from newly developing nuclear models. It is also necessary for determining the nuclear skin with good accuracy.

1.1 Glauber model of CCCS

It is important that we have a theory to determine proton radii from CCCS with reasonable precision. In the following we present the new theory which works very well for all of known CCCS and proton radii.

In the Glauber calculations of reaction cross sections, only z-integrated density distribution of a nucleus comes into the equations. We write the z-integrated density distributions of a projectile and a target as,

$$\rho_{Pm}(r) = \rho_{Pp}(r) + \rho_{Pn}(r)$$
$$\rho_{Tm}(r) = \rho_{Tp}(r) + \rho_{Tn}(r) \quad .$$

were r is the two-dimensional distance from the center of a nucleus. Indices P and T are for the projectile and target nuclei, and p and n are for proton and neutron, respectively.

The interaction cross section (σ_I) is calculated, under the optical limit (or single scattering approximation), as

$$\sigma_I = \int [1 - T(b)] d\mathbf{b}$$

where the transmission function at impact parameter b, $T(b)$, is written as,

$$T(\mathbf{b}) = \exp[-\sigma_{pp} \int \{\rho_{Pp}(\mathbf{r}-\mathbf{b}) \cdot \rho_{Tp}(\mathbf{r}) + \rho_{Pn}(\mathbf{r}-\mathbf{b}) \cdot \rho_{Tn}(\mathbf{r})\} d\mathbf{r}$$
$$- \sigma_{pn} \int \{\rho_{Pp}(\mathbf{r}-\mathbf{b}) \cdot \rho_{Tn}(\mathbf{r}) + \rho_{Pn}(\mathbf{r}-\mathbf{b}) \cdot \rho_{Tp}(\mathbf{r})\} d\mathbf{r}] \quad .$$

It is essentially the overlap integral of the projectile and the target densities multiplied by the nucleon nucleon cross sections σ_{pp} and σ_{pn}. [$\sigma_{pp} = \sigma_{nn}$]

To calculate transmission function for the charge changing cross section $T_c(b)$, only the transmission through protons in the projectile should be taken into account. Therefore,

$$\sigma_{cc} = \int [1 - T_c(b)] d\mathbf{b}$$
$$T_c(\mathbf{b}) = \exp[-\sigma_{pp} \int \rho_{Pp}(\mathbf{r}-\mathbf{b}) \cdot \rho_{Tp}(\mathbf{r}) d\mathbf{r} - \sigma_{pn} \int \rho_{Pp}(\mathbf{r}-\mathbf{b}) \cdot \rho_{Tn}(\mathbf{r}) d\mathbf{r}] \quad .$$

However this equation is not valid because a distortion of the target nucleus by the neutrons in the projectile is not included. This is the effect due to the scattering of the target nucleons by a neutron in the projectile before scattering with a proton in the projectile. To take into account this effect, the attenuation factors are introduced. Then the densities of the target should be replaced by the distorted densities,

$$\rho_{Tp}(\mathbf{r}) \rightarrow \exp[-\lambda\sigma_{pn}\rho_{Pn}(\mathbf{r}-\mathbf{b})]\cdot\rho_{Tp}(\mathbf{r})$$
$$\rho_{Tn}(\mathbf{r}) \rightarrow \exp[-\lambda\sigma_{nn}\rho_{Pn}(\mathbf{r}-\mathbf{b})]\cdot\rho_{Tn}(\mathbf{r})$$

Here the exponential factors are attenuation of the proton and the neutron in the target by the collision with neutrons in the projectile. λ here is the parameter to control the mean free path effect before interacting with protons in the projectile. This parameter provides the effective factor of change of the target densities to fit the real data. It depends on, for example, an incident energy because of the change in angular distribution of N-n scattering. At high energy, scattering is strongly forward peaked so that the N-n scattering does not change the path of N very much and thus attenuation of the density is not significant. However at a low energy, the scattering changes the direction of N significantly and thus distortion is stronger.

Firstly we test this model with symmetric stable nuclei, ^{10}B, ^{12}C, ^{14}N, ^{16}O, ^{20}Ne, of which CCCS have been determined with high precisions. In those nuclei, the proton distributions are same as the neutron distributions. Therefore the relation between σ_I and σ_{cc} would provide the coefficient λ. In particular at high energy such as 800A MeV, λ~0. Figure 4 shows such relations, Square dots (blue) are σ_I, Round circles (red) and triangles (green) are σ_{cc} of those nuclei at high energies incident on Carbon target. (800A and 950A MeV). The former is by Chulkov et al., [7] and the latter is by Webber et al. [8]. As mentioned already, they are not consistent with each other. The energy difference in these experiments does not lead to such significant change in cross section. The line (purple) is the Glauber model charge changing cross sections using the density distributions determined by the σ_I assuming $\rho_p(r) = \rho_n(r)$. The λ=0 was used and harmonic oscillator type densities were used. It agrees very well with Webber's values.

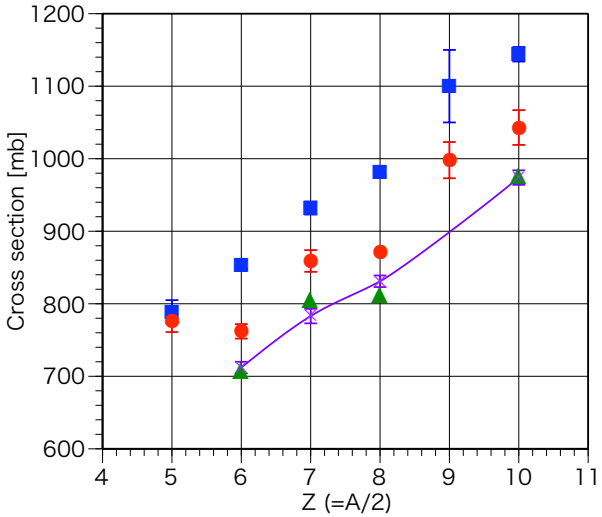

Fig. 4 Interaction cross sections and charge changing cross sections.

Concerning the neutron rich nuclei, so far both of the isotope shift and the CCCS have been measured only for ^{8,9,11}Li. Therefore we use the interaction cross section, the CCCS, and the charge radius of ^{8}Li to determine the λ for the energy of CCCS measurement (80A MeV). The λ was determined to be 0.68 for this case. Assuming that the λ is equal for all Li isotope measurements, we found the proton and the neutron density distribution (harmonic oscillator type) that consistently reproduce the σ_I and σ_{cc} simultaneously. Thus determined rms radii of proton distributions are shown in Table I ($\langle r_p^2\rangle^{1/2}_{from\ cc}$) together with the proton radii determined by isotope shift measurements, $\langle r_p^2\rangle^{1/2}_{exp}$. Agreements are impressive showing that the proton rms radii can be determined well from the CCCS.

Table I. The interaction and charge changing cross sections and proton rms radius of Li isotopes.

	σ_I	σ_{cc}	a_p	a_n	$\langle r_p^2\rangle^{1/2}_{exp}$	$\langle r_p^2\rangle^{1/2}_{from\ cc}$
8Li	768±9	510±20	1.69	1.76	2.16±0.01	fit
9Li	796±6	470±10	1.59	1.754	2.08±0.02	2.05±0.04
11Li	1056±14	510±30	1.765	2.28	2.37±0.02	2.30±0.11

a_p and a_n are harmonic oscillator size of proton and neutron distribution, respectively.

2. Proposed experiment

Charge changing cross sections (CCCS) of $^{8\text{-}17}$B, $^{9\text{-}20}$C, $^{13\text{-}24}$O isotopes on C target will be measured at around 900*A* MeV. The goal is to determine the cross sections with precision ~ 1.5%. The beams of stable isotopes like ^{12}C, ^{16}O will provide a test of the method since the proton radii of these isotopes are well determined.

The CCCS will be measured by the transmission method. The cross section is determined as,

$$\sigma_{cc} = \frac{1}{t}\ln\left[\frac{\gamma_0(1-P_m)}{\gamma}\right], \quad (1)$$

where t is the number of target per [cm^2] and

$$\gamma = N_{sameZ} / N_{inc}\,. \quad (2)$$

is the ratio of number of incident nucleus (N_{inc}) and the number of out-going nuclei with same atomic number Z (N_{sameZ}). γ_0 is the same ratio in the measurement without target. (1-P_m) is the correction factor for the number of nuclei scattering out of detectors after the target. The main advantage of the method is the event by event selected counting of the incident beam. Therefore no uncertainty exists in N_{inc}. The number of unchanged charge event (N_{sameZ}) will be determined from counting the number of detected nuclei that have same Z as the incident nuclei. This is better than counting the number of nuclei with Z different from that of incident nuclei. The reaction may be extremely violent and thus no particle may hit the detector after the target. P_m is the correction due to the scattering out of the nuclei that has unchanged Z after the target. The probability of the scattering out is considered to be very small (0.1%) but will be estimated from the position (or angular) distribution of same Z nucleus determined.

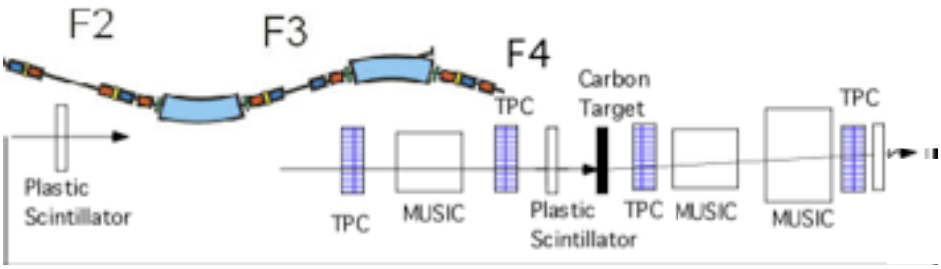

Fig. 5 Schematic view of experimental setup at F2 and F4.

The measurements are straight forward and the analysis of the data is not complicated so that the results might be obtained quickly.

3. Experiment Conditions

The experiment will be performed at the final focus F4 of the fragment separator, FRS. A schematic view of the proposed experimental setup is shown in Fig.5. The secondary beam will be identified using the magnetic rigidity (Bρ), time-of flight(TOF) and energy-loss(ΔE). The TOF will be measured between the two plastic scintillators located at F2 and F4. The energy loss will be measured using the first multi-sampling ionization chamber (MUSIC) at F4. The slits ±10mm used at F4 are meant for restricting the contaminant particles. The Time Projection Chamber (TPC)

detectors provide beam tracking at F4 and also provide additional measure of energy-loss that can be used for reducing the background in the incident beam.

The Carbon reaction target will be located after the S4 plastic. The reaction products with the same charge as the incident beam will be identified using two multi sampling ionization chambers. To make the mixing of the tail of the other charge less than 1/1000, the ΔE resolution (σ) of the detector should be better than (ΔE(Z=8)- ΔE(Z=7))/3.7 assuming that the ΔE spectra are Gaussian distribution. The pulse height difference of O and N is about 23% and thus the requirement is σ<6% The MUSIC detectors have a Z-resolution of ~ 3% for O isotopes. For the purpose of measuring the charge changing cross section, no mass identification is necessary.

The use of two MUSICs after the target together with tracking and scintillator detectors will allow us to accurately determine the detection efficiency. The tracking detectors behind the target allow us to determine the angles of the fragments with same Z as the incident beam.

The experiment will be performed for the entire isotopic chains of B, C and O. The primary beam intensity will be the highest available one for producing the very neutron-rich isotopes, as well as for the proton drip-line isotopes. In the intermediate region the primary beam intensity will be reduced in order to maintain a total rate <5x10^5/sec on the plastic scintillator at F2 and a total rate of 3x10^3/sec on the plastic scintillator at F4. The latter will determine the trigger rate for the experiment and hence the limit comes from having a measuring condition without appreciable dead time.

To estimate and eliminate effects of reactions in non-target material, data will be collected for each isotope without the reaction target.

The estimation for beam time is based on secondary beam intensities expected using a simulation of beam transport through the FRS and production cross sections as predicted by EPAX.

The required intensity of the secondary beams are obtained from the optimization of desired statistical accuracy required for the experiment. Our aim is to achieve close to 1.5% uncertainty in order to be close in precision to the interaction cross section measurements. This will allow us to determine the skin thickness precisely as well as determine the evolution pattern of charge radius for each isotopic chain.

3.1 Uncertainty of the measured cross section

In a transmission type measurement with no uncertainty of the number of incident nuclei, the error of the cross section $\Delta\sigma_{cc}$ can be calculated as,

$$\left(\frac{\Delta\sigma_{cc}}{\sigma_{cc}}\right)^2 = \left\{\frac{1-\gamma}{N_{inc}\gamma} + \frac{1-\gamma_0}{N_{0inc}\gamma_0} + \left[\frac{\Delta(\gamma/\gamma_0)}{\gamma/\gamma_0}\right]^2 + \left[\frac{\Delta(1-P_m)}{(1-P_m)}\right]^2\right\}\left(\frac{1}{\sigma_{cc}t}\right)^2 + \left(\frac{\Delta t}{t}\right)^2 \quad (3)$$

where subscript 0 indicates the quantities measured when the target is out. The first two terms comes from the statistics under the binomial distribution, not a Gaussian distribution, and the second term is due to the uncertainty of the identification of Z after the target. The fourth term is the uncertainty of the scattering-out probability. The last term is the uncertainty of the target thickness.

To understand the effect of statistics on the error we explain the error for special case where no other uncertainties affect the final error; γ0=1, Pm=0. The statistical error for charge changing cross sections is, then, written as,

$$\frac{\Delta\sigma_{cc}}{\sigma_{cc}} = \frac{1}{\ln\gamma}\sqrt{\frac{1-\gamma}{\gamma}}\frac{1}{\sqrt{N_{inc}}} . \quad (4)$$

Figure 6(a) shows the statistical error for different N_{inc} and target thickness conditions. The total error, assuming the systematic uncertainty to be 1.2% is shown in Fig.6(b). The calculations are done for σ_{cc} = 500 mb. It is seen that for each beam condition the error dependence on target thickness is rather flat after a certain thickness. Therefore using thicker targets than this value is not meaningful. Thinner targets (as much as possible) will be preferable to keep multiple scattering effects minimized. The optimized condition is obtained with a total of 10^5 incident beam particles and a target thickness of 4 g/cm^2.

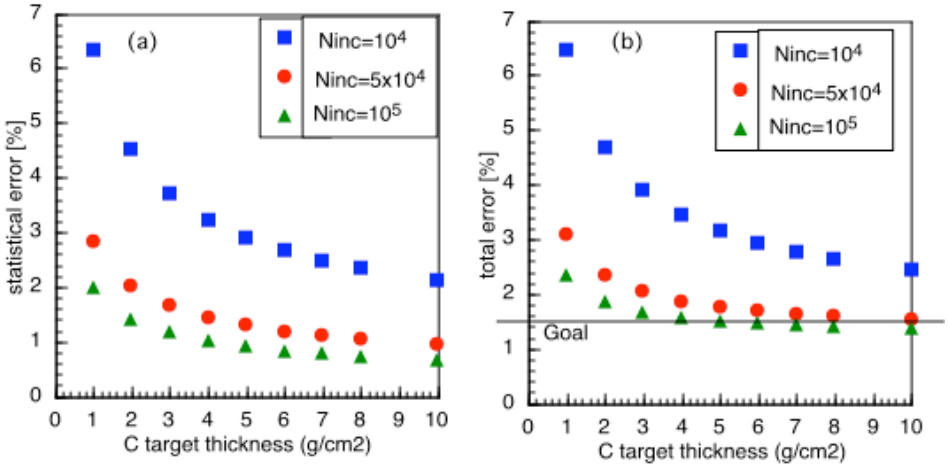

Fig.6 (a) The statistical uncertainty estimated as a function of Carbon target thickness for different number of incident nuclei (squares : 1e+4, circles:5e+5, triangles:1e+5). (b) The total uncertainty that includes the statistical uncertainty and an uncertainty of 1.2% for systematic uncertainty. The symbols are same as in (a).

3.2 Beam intensities and beamtime

With the goal to achieve 10^5 incident nuclei on the reaction target the data taking time required for the individual isotopes are shown in Table 1. The estimated rate of the secondary beam on reaction target with highest primary beam intensities are shown in Fig.7.

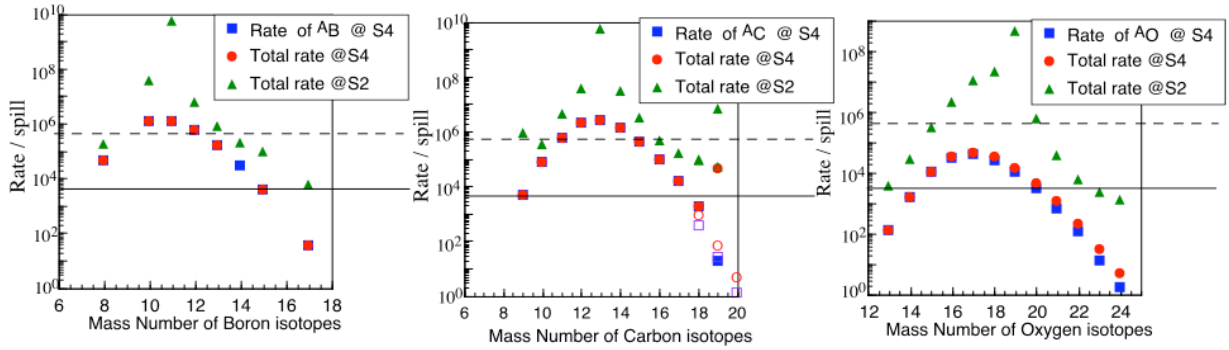

Fig.7 The rates/spill as estimated using simulations for beam transport through FRS. The Left, middle, right graphs are for B, C and O isotopes respectively. The primary beam intensities considered are ^{22}Ne : 1e+10/spill, ^{40}Ar : 6e+10/spill, ^{48}Ca: 1e+9/spill. The dashed lines/solid lines show the limit that we can allow for total rates at S2/S4. The primary beam intensities for cases that are above the dashed and solid lines will have to be reduced such that the rates are below those lines.

The primary beam energy is chosen to be 1*A* GeV in order to ensure firstly the best forward focussing of particles allowing complete detection. Secondly the Glauber model analysis will be best suited at energies > 800 MeV where the nucleon-nucleon cross section has a flat energy dependence. Finally it is necessary to have the interaction and charge changing cross section measured at similar energies.

The rates shown (Fig.7) are expected using a slit of ±10mm at S4 and a 6g/cm^2 achromatic Aluminum wedge degrader at S2.

Table 2 presents a summary of the estimated time that will be necessary for each measurement. In this estimate we have considered, where necessary, reduced primary beam intensities to keep the total rate at S2 and S4 below the dashed and solid lines (Fig.6).

Table 2: Summary of beamtime request

Jobs	Primary beam	Secondary Beam	Time per isotope (hours)	Total time (hours)
σ_{cc}–data taking (target-in + target-out)	^{22}Ne	$^{8\text{-}15}$B	1.5	12
σ_{cc}–data taking (target-in + target-out)	^{22}Ne	^{17}B	4	4
σ_{cc}–data taking (target-in + target-out)	^{22}Ne	$^{9\text{-}17}$C	1.5	13.5
σ_{cc}–data taking (target-in + target-out)	^{40}Ar	^{18}C	1.5	1.5
σ_{cc}–data taking (target-in + target-out)	^{40}Ar/^{22}Ne	^{19}C	5	5
σ_{cc}–data taking (target-in + target-out)	^{40}Ar	^{20}C	93	93
σ_{cc}–data taking (target-in + target-out)	^{48}Ca	$^{13\text{-}21}$O	1.5	13.5
σ_{cc}–data taking (target-in + target-out)	^{48}Ca	^{22}O	2.5	2.5
σ_{cc}–data taking (target-in + target-out)	^{48}Ca	^{23}O	10	10
σ_{cc}–data taking (target-in + target-out)	^{48}Ca	^{24}O	68	68
Magnet settings (target-in + target-out)			1	37
Intial calibrations and setup with beam				24
Total beamtime				284 ~ **36 shifts**

3.3 Concern on the proton dripline nuclei

It is clear that the charge changing cross section is equal to the interaction cross section for a proton dripline nucleus. Even if only a neutron is knocked out by the reaction, proton(s) is evaporated because it is outside the dripline. In general, a proton rich nuclei have a smaller proton separation energy than that of neutrons. Then proton(s) may be evaporated after the knock out of

neutron by the reaction. Therefore CCCS will be larger than the geometrically expected cross sections. We will, however, like to measure CCCS for proton rich nuclei for estimating this evaporation effect to extrapolate to the neutron rich nuclei.

References :

[1] Y. Kanda-En'yo, Phys, Rev. C 71 (2005) 014310.

[2] L. -B Wang et al., Phys. Rev. Letters 93 (2004) 142501.

[3] R. Sanchez et al., Phys. Rev. Letters 96 (2006) 033002.

[4] T. Suzuki et al., Phys Rev. Letters 75 (1995) 3241.

[5] H. Drake et al., Phys. Rev. A **65** (2002) 054501.
D. Das and V. Natarajen, Phys. Rev. A **75** (2007) 052508.

[6] B. Blank et al., Zeitschrift fur Physik A, Hadrons and Nuclei 343, 375-379

[7] L. V. Chulkov et al., Nucl. Phys. A 674 (2000) 330.

[8] W.R. Webber, J.C. Kish and D.A. Schrier Phys. Rev. C 41 (1990) 520.